THE SOLUTION RATE AND RECOVERY OF FERROALLOYS

Dr. Stavros A. Argyropoulos
Iron and Steel Society Professor
Dept. of Metallurgy and Materials Science
University of Toronto
184 College Street , Toronto , Ontario M5S 1A4
CANADA

ABSTRACT

Factors affecting the solution rates and recoveries of ferroalloys are examined and analysed. The various routes which different ferroalloys follow during their assimilation into liquid steel and in high carbon liquid iron are presented and analysed. A modern experimental technique for the characterization of solution rates of ferroalloys is shown. Using this technique more than 50 different ferroalloy grades have been examined. Representative results are given.The role as well as the type of the exothermicity in the solution rate are presented.

INTRODUCTION

The precision which the modern steelmaking practice requires has resulted in more careful ferroalloy addition practices. These practices require that the ferroalloy additions must exhibit repeatable and consistently high recoveries. Certainly, the steelmaking practice plays a part in determining final recovery rates as well as the degree of deoxidation of the heat, turbulence in the ladle, and a number of other factors. What is most important, however is the physicochemical properties of the ferroalloy itself. Recovery depends upon the physicochemical properties of ferroalloy such as its solution rate and density, as well as the dissolved oxygen in liquid steel. The above-mentioned can be expressed mathematically as follows:

$$R = f(u, \rho, [O]) \qquad (1)$$

where R : recovery
u : solution rate
ρ : density
[O] : dissolved oxygen in liquid steel

It must be emphasized that equation (1) is not directly applicable to ferroalloys which are used as nitrogen scavengers, like the 18 wt% Ferroboron. The solution rate is the single most important property determining a ferroalloy's recovery. The faster an alloy can go into solution, the less chances exist for losses. Almost as important as solution rate is the alloy addition density. The ideal ferroalloy should have a density in the range : from 6.2g/cm^3 to 7.6g/cm^3. However, if the steel bath is not deoxidized well, then the recovery can be low even if the ferroalloy has a high solution rate and an ideal density.

The transfer of ferroalloy additions from a solid to a liquid can be characterized as melting or dissolution. The former occurs when heat is applied, while the latter takes place when the solid material comes in contact with a liquid at temperatures below the melting point of the solid. The dissolution process may be divided into two consecutive steps. The first step is the surface reaction in which the solid goes through a phase change to the liquid. The second step is the transporting of the resulting solute atoms from the interface into the bulk of liquid steel by diffusion through a boundary layer. Either step can be rate-controlling in the dissolution.The ferroalloy additions in liquid steel can be classified into two classes: class I includes those additions with a melting range lower than that of liquid steel temperatures; class II refers to those additions with melting ranges higher than that of liquid steel temperatures.

In this paper the solution of ferroalloys in liquid steel will be characterized as melting for class I ferroalloys and as dissolution for class II ferroalloys. Factors affecting recoveries and solution rates of ferroalloys will be examined and analysed. A modern experimental technique for the identification of solution rates of ferroalloys will be shown.

ASSIMILATION ROUTES

Figure 1 shows the various assimilation routes that would be observed during the

assimilation of a ferroalloy in liquid steel. In this figure, the ferroalloys were considered to be spherical . On the cold ferroalloy (Route 1A), a steel shell solidifies (Route 1B) immediately upon immersion. This shell subsequently grows, and the inside ferroalloy begins to melt (Route 1C). When the shell melts back, the inside ferroalloy is in a molten state that is then assimilated into the liquid steel (Route 1D). This route is observed in cases of low steel bath superheats. Figure 2 depicts a ferromanganese cylinder made for the identification of various routes. Figure 3 shows a cross section of a similar ferromanganese cylinder following this route.

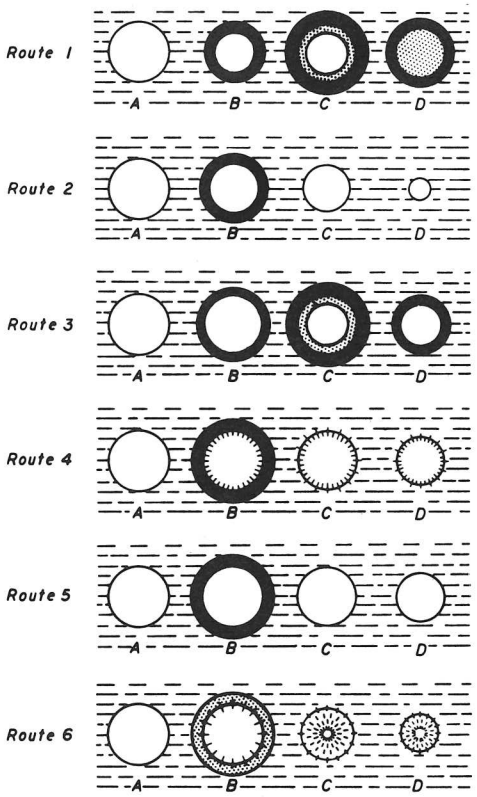

Figure 1: Assimilation routes of various ferroalloy lumps into liquid steel

In Route 2 and at the point where the steel shell melts back, the ferroalloy addition is very close to its melting point and the periods (Route 2C and 2D) are very short. Conditions favoring Route 2 include high superheat temperatures (80°-100°C) and large lumps with low thermal conductivities.

Referring to Route 3, the steel shell freezes (Route 3B) and then melts back (Route 3C) and a second shells solidifies around the remaining unmelted portion of the ferroalloy. Favorable conditions for this route include extremely high

Figure 2: Picture of ferromanganese cylinder 3.8 cm in diameter and 15.2 cm in length.

superheats (≈130°C and higher), low thermal conductivity and large lumps. In Figure 4, the left

Figure 3: Cross section of a ferromanganese cylinder following immesion for 30 seconds in a steel bath having initial superheat of 30°C. Initial cylinder diameter was 3.81 cm.

cylinder shows the initial cross section prior to immersion, whereas the right cylinder shows the final cross section after immersion for 20 seconds

in a liquid steel with extremely high superheat. It is clear that the cylinder on the right is surrounded by a steel shell and that its cross section is smaller than that of the cylinder on the left. These cross sections confirm the second shell formation route, which is depicted by route 3 in Figure 1.

Figure 4: The cylinder on the left is shown before immersion in liquid steel, and on the right is a cross section of a similar ferromanganese cylinder following immersion for 20 seconds in a steel bath having an initial superheat of 130°C. Initial cylinder diameter was 3.81 cm.

Pointing in the forth route a reaction occurs at the steel shell ferroalloy interface (Route 4B). This reaction accelerates the normal melting phenomena. The rate of acceleration depends upon the degree of the exothermicity a particular ferroalloy exhibits when it is assimilated into liquid steel. Notable examples include silicon and different grades of ferrosilicon alloys. Figures 5 , 6 , and 7 show cross sections of 3.81 cm 50wt% Ferrosilicon cylinders immersed in liquid steel for 5, 10, and 15 seconds respectively. The cylinders were then retrieved and sectioned. As seen , there is no trace of reaction for the cylinder which was immersed in liquid steel for 5 seconds (i.e. Figure 5) . The reaction zone becomes progressively thicker for the cylinders immersed for 10 and 15 seconds (i.e. Figures 6 and 7).

In the fifth transfer Route, a steel shell first solidifies around a ferroalloy then the steel shell melts back, and a dissolution process follows

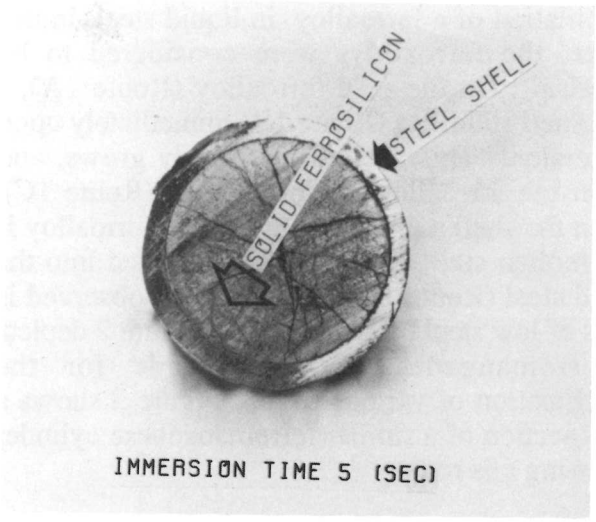

Figure 5: Sectioned 50 wt% ferrosilicon cylinder showing encasing steel shell and extent of reaction zone following immersion for 5 seconds.

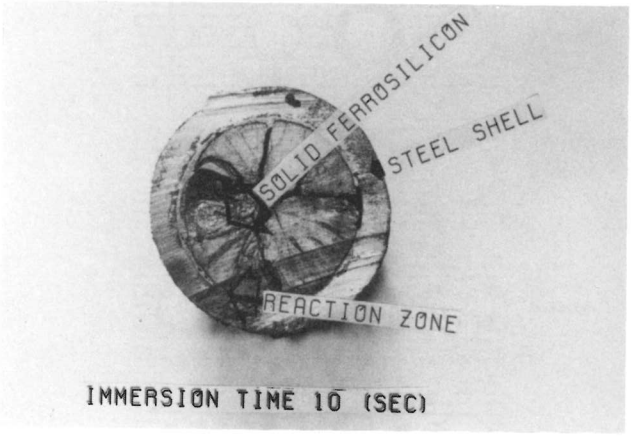

Figure 6: Sectioned 50 wt% ferrosilicon cylinder showing encasing steel shell and extent of reaction zone following immersion for 10 seconds.

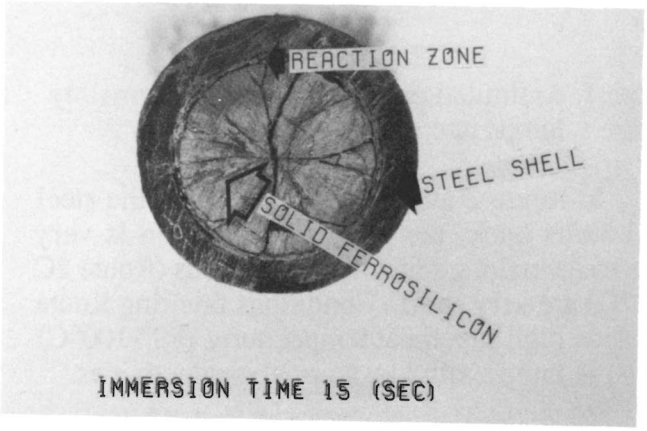

Figure 7: Sectioned 50 wt% ferrosilicon cylinder showing encasing steel shell and extent of reaction zone following immersion for 15 seconds.

(Routes 5C and 5D) . The dissolution period is longer than the steel shell period. This route is followed by ferroalloys that have melting ranges above liquid steel temperatures and do not exhibit any exothermicity with liquid steel. Typical examples of ferroalloys that follow this route include 80wt% ferrovanadium, ferrotungsten, ferromolybdenum and ferroniobium.

Referring to the sixth transfer Route, a steel shell freezes around the addition (Route 6B). The steel shell then melts back and a reaction occurs (Route 6C). This reaction is a result of the formation of an intermetallic compound which is usually associated with a certain amount of heat release. This heat is called "Microexothermicity" and alters the whole assimilation process from dissolution to melting. The term "Micro-exothermicity" was coined in an earlier work to indicate the type of exothermicity which will be released when the intermetallic formation in powder alloy compacts take place (1). This Route occurs in briquetted ferroalloy compacts and it has been observed in liquid steel and high carbon liquid iron (2). Figure 8 depicts a typical microexothermic briquette from ferroniobium.

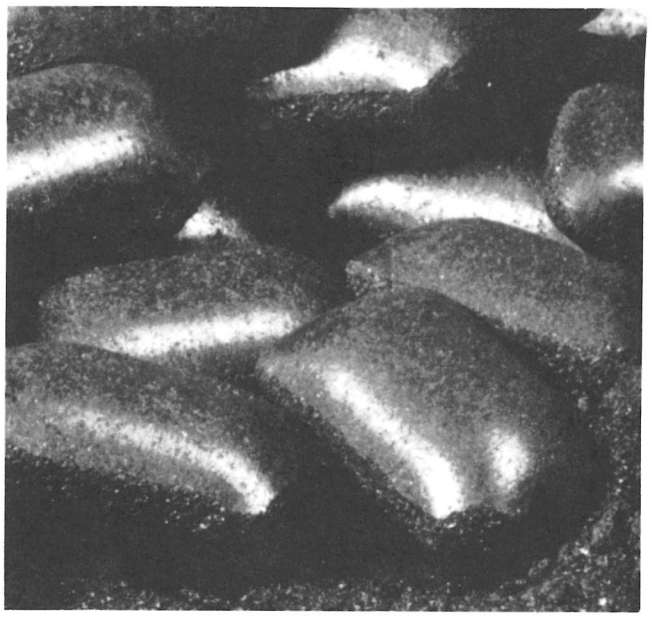

Figure 8: Typical microexothermic ferroniobium briquette.

The various grades of ferrovanadium lumps exhibit different assimilation routes when they are immersed in the liquid steel.The ferrovanadium grades with low vanadium content follow one of the first three routes during their assimilation into liquid steel.The grades with high vanadium content (i.e. 80 wt% Ferrovanadium) follow route five.Figure 9 shows the mass transfer mechanisms for various grades of ferrovanadium alloys. More details on the ferrovanadium alloys can be found in reference 3.

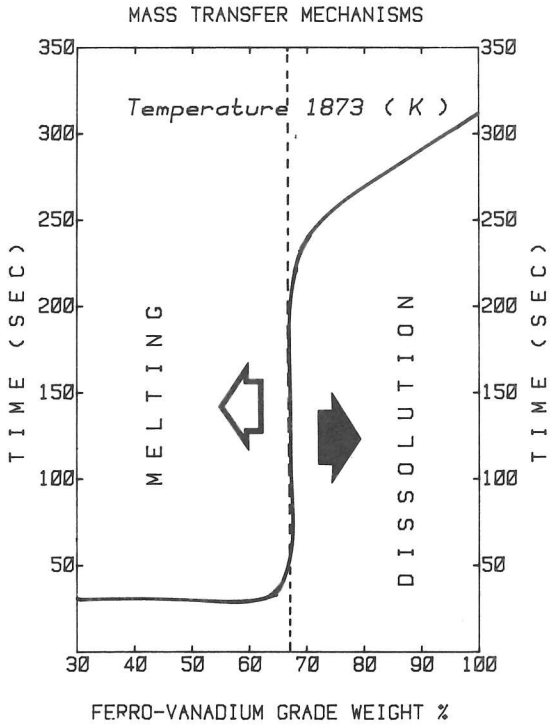

Figure 9: Predicted melting/dissolution times required for 2.54 cm diameter cylinders of ferrovanadium versus ferrovanadium grade to disperse into liquid steel at 1600°C.

DYNAMIC CHARACTERIZATION OF SOLUTION RATE

An experimental technique was developed which enables the measurement of solution rate of ferroalloys in a "Dynamic way". In this technique, a smooth and oblong ferroalloy lump is immersed into liquid steel and the apparent weight of the lump is measured with a load cell. Figure 10 presents a schematic cross section of the induction furnace where 65 kg of steel are melted. The temperature of the steel bath is measured with a thermocouple which is continuously immersed into liquid steel. The analog outputs from the bath thermocouple and the weight sensor are fed to a microprocessor based intelligent measurement system which records in real-time. Figure 11 shows a schematic layout of this system. The interested reader can find more details on this system in reference 4. Using similar configurations shown in figures 10 and 11 , the solution rates of more than 50 different ferroalloy grades have been examined.

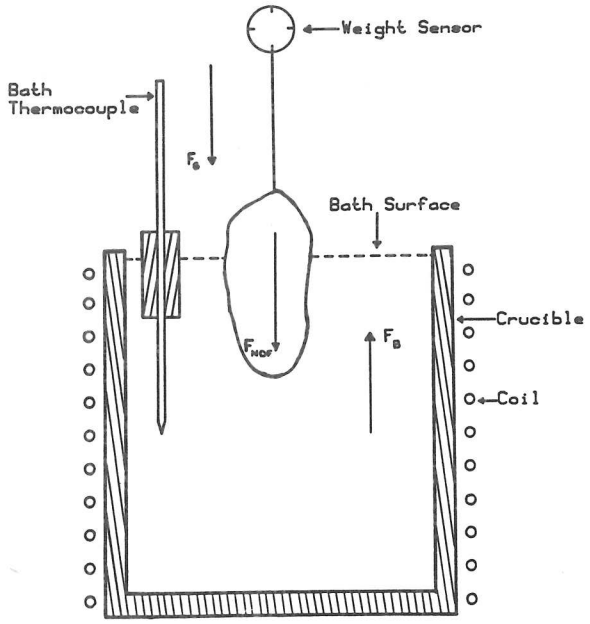

Figure 10: Schematic cross section of an induction furnace with the ferroalloy lump, bath thermocouple and weight sensor.

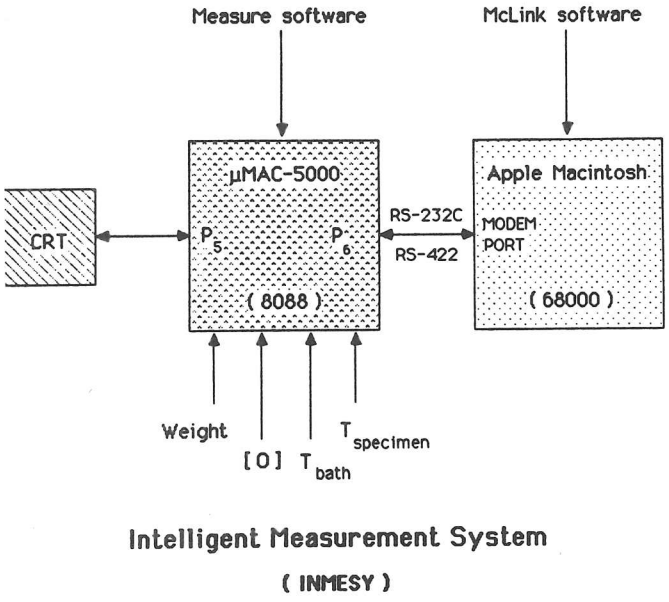

Figure 11: Schematic layout of the intelligent measurement system (INMESY).

Figures 12, 13, and 14 present some representative results from these tests. In all of these figures, curve 1 represents the measured temperature of the steel bath during immersion of the ferroalloy lump, with the temperature shown in

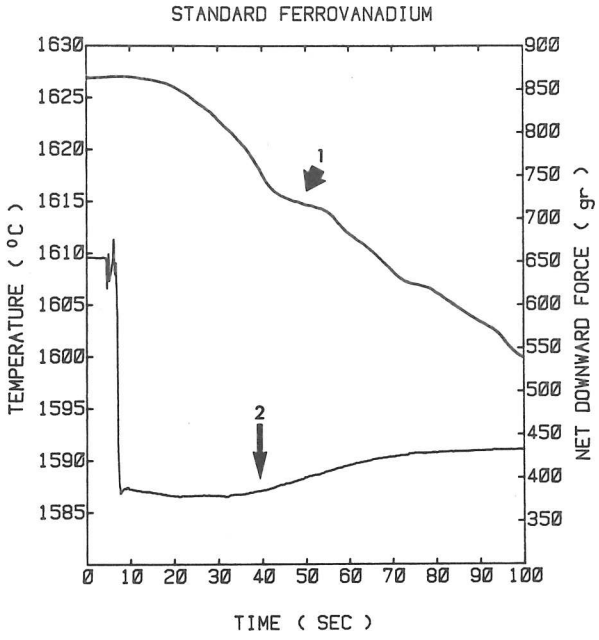

Figure 12: Solution of 66 wt% ferrovanadium in liquid steel. Curve 1 shows the measured steel bath temperature. Curve 2 presents registered net downward force.

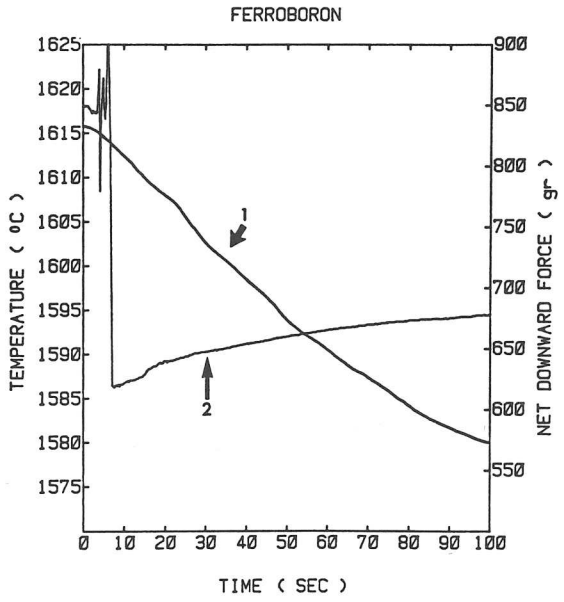

Figure 13: Solution of 17 wt% Ferroboron in liquid steel. Curve 1 shows the measured steel bath temperature. Curve 2 presents registered net downward force.

the left of the Y-axis. Curve 2 denotes the registered net downward force during the

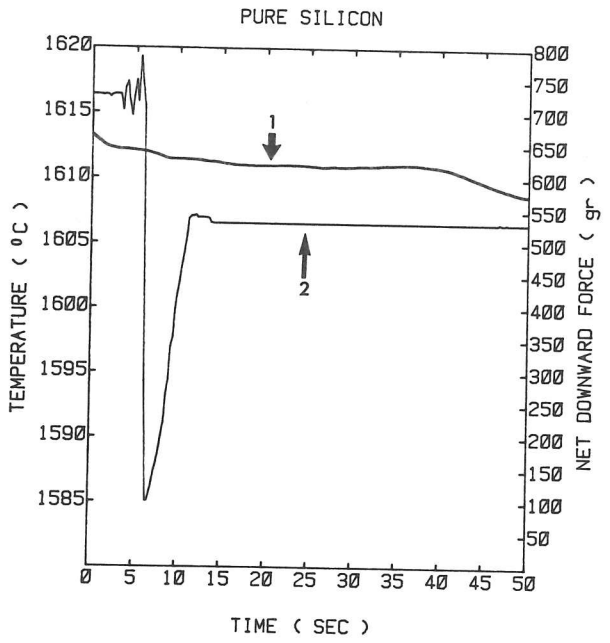

Figure 14: Solution of Silicon metal in liquid steel. Curve 1 shows the measured steel bath temperature. Curve 2 presents the registered net downward force.

immersion and is shown on the right of the Y-axis. Examining the various segments of curve 2 the solution rate of the ferroalloy can be evaluated. The interested reader can find more details on the dynamic characterization of solution rates of ferroalloys in references **5,6,7** and **8**.

This technique was also used for measurements of solution characteristics of various ferroalloys in carbon saturated liquid iron (2). More recently, Cored-Wire Microexothermic ferroalloys for tundish metallurgy were developed using the experimental technique discussed above (9). These facts demonstrate the versatility of this technique for a variety of immersion objects in various liquid media.

SOLUTION RATES AND RECOVERIES IN LIQUID STEEL

The Effect of Oxygen

An important factor which influences the recovery of alloys is the dissolved or active oxygen content in molten steel. The measurement of dissolved oxygen content is, thus, the only way to solve the steel production equation: how much, and sometimes what, ferroalloys to use to obtain as clean, castable and optimum steel as possible at minimum cost. Conditions of ladle metallurgy stations were simulated in an induction furnace, where the effects of oxygen on the recovery and solution speed of ferroalloys were studied under pilot scale conditions. Figure 15 presents a schematic cross-section of the experimental apparatus. Based on the experimental results, statistical equations were derived where the recovery and the solution speed are given as a function of dissolved oxygen in liquid steel.

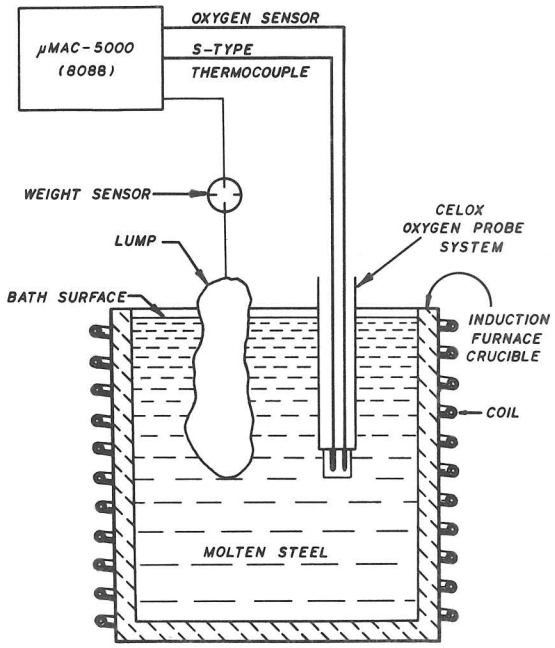

Figure 15: Schematic cross section of the induction furnace with ferroalloy lump, weight sensor, Celox oxygen probe system, and the intelligent satellite micro-peripheral μMAC-5000.

Figure 16 shows the experimental results for ferromanganese where the measured recovery is plotted against the measured active or dissolved oxygen of the steel bath. A linear regression analysis of these results was performed in order to deduce the relationship between the recovery of Manganese and the dissolved oxygen in the steel bath. The equation for curve 1 in Figure 16 is:

$$R_{Mn} = 77.2 - 0.05\ [O] \qquad (2)$$

where [O] is the dissolved oxygen in ppm with a correlation coefficient of 0.931 with 8 degrees of freedom and a standard error of estimate of 6.95.

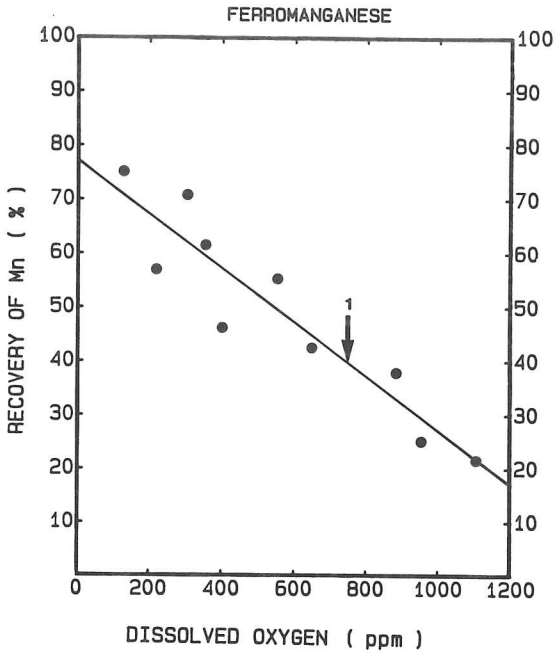

Figure 16: Recovery of ferromanganese lumps as a function of active or dissolved oxygen in liquid steel. Curve 1 shows the regression line.

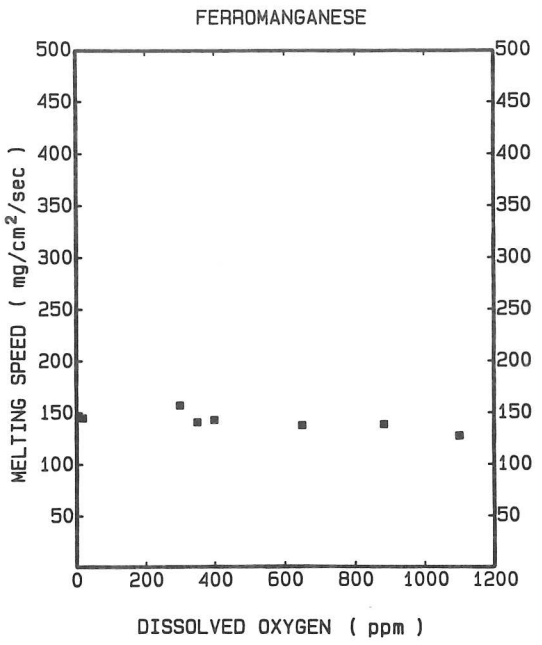

Figure 17: Melting speed of ferromanganese lumps as a function of dissolved or active oxygen in liquid steel.

Similar tests for silicomanganese were performed and equations 3 and 4 present the results for the recoveries of manganese and silicon, respectively, of the silicomanganese ferroalloy.

$$R_{Mn} = 77.1 - 0.035\ [O] \quad (3)$$

$$R_{Si} = 83.0. - 0.075\ [O] \quad (4)$$

For 75wt% grade Ferrosilicon

$$R_{Si} = 71.2 - 0.049\ [O] \quad (5)$$

For Silicon metal

$$R_{Si} = 81.5 - 0.044\ [O] \quad (6)$$

For Standard grade Ferroniobium

$$R_{Nb} = 70.48 - 0.045\ [O] \quad (7)$$

Figure 17 shows the effect of dissolved oxygen on the melting speed of ferromanganese lumps. As seen, the dissolved oxygen in liquid steel has no significant effect on the melting speed . Similar results were observed for silicomanganese and silicon metal lumps. The interested reader can find more details on this research in reference **6**. Figure 18 presents the effect of dissolved oxygen on the dissolution speed of standard ferroniobium alloys.

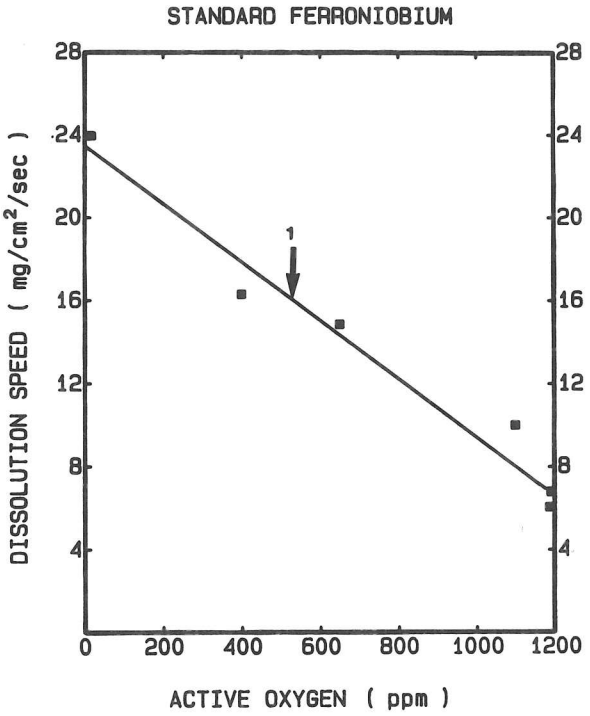

Figure 18: Dissolution speed of standard grade Ferroniobium lumps as a function of dissolved oxygen in liquid steel.

In this case the dissolved oxygen has significant effect on the dissolution speed. In the case of 80wt% ferrovanadium similar effects with the ones

noticed for standard ferroniobium were also observed (6).

From the results shown in the previous equations, it appears that the complex deoxidizers (i.e. silicomanganese) exhibit better recovery performance. For example, the expected recovery of manganese from a ferromanganese ferroalloy, which was used in a steel bath with a dissolved oxygen of 500 ppm, can be derived from equation 2 and is equal to 52.2%. On the other hand, if a silicomanganese ferroalloy was used under the same steel bath conditions, dissolved oxygen of 500 ppm, then the expected recovery of manganese is given by equation 3 and is equal to 59.6%. Obviously the above improvement was achieved at the expense of silicon recovery. In this case the

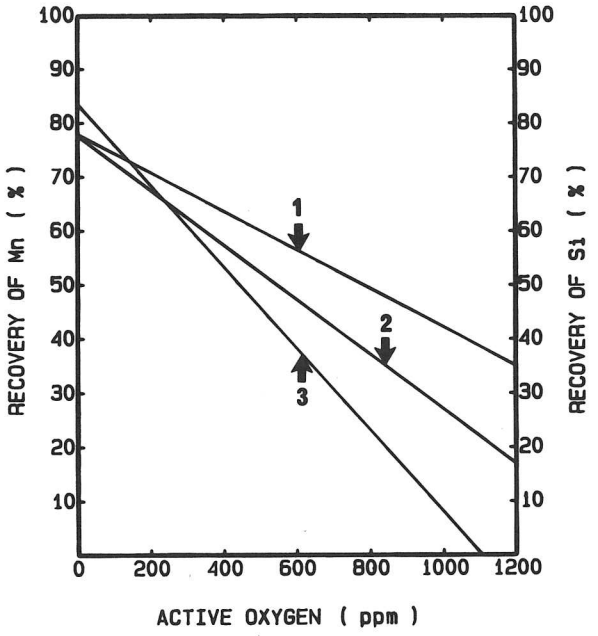

Figure 19: Expected recoveries of silicomanganese alloys. Line 1 and line 3 show the expected recoveries of Manganese and Silicon respectively in silicomanganese ferroalloys. Line 2 depicts the expected recovery of Manganese in ferromanganese ferroalloys.

calculated silicon recovery from equation 4 is 45.5%. Figure 19 shows equations 2, 3 and 4 in a graphical form. Line 1 depicts equation (3) which presents the recovery of Manganese from silicomanganese lumps. Line 2 shows equation (2) which depicts the recovery of Manganese from ferromanganese lumps. Line 3 represents equation (4) which presents the recovery of Silicon from silicomanganese lumps. As seen in Figure 18, the gap between curves 1 and 2 increases at a higher dissolved oxygen content. This means that at this higher content, the expected recoveries of manganese would be higher if silicomanganese were used instead of ferromanganese.

Another important conclusion derived from these results is that the dissolved oxygen has no effect on the melting speed of class I ferroalloys. This can be explained by the fact that for these types of ferroalloys, their assimilation into liquid steel is heat transfer controlled. However, quite the opposite situation was observed for class II ferroalloys. As seen from the case of standard ferroniobium, the solution speed is largely affected by the dissolved oxygen in liquid steel. This can be explained by the fact that this ferroalloy follows a dissolution mechanism and consequently its assimilation into liquid steel is very slow. Since the ferroniobium and 80wt% ferrovanadium have very slow dissolution kinetics, they have a greater chance of forming solid refractory oxides whenever they are used in a steel bath with a high dissolved oxygen content. This in turn might reduce their effective dissolution speed.

In the cases of alloying steel baths with high dissolved oxygen contents, the recently developed family of microexothermic (Autoexothermic) ferroalloys can be used as a viable alternative.(1) The silicon modifier in these compacts would have a dual role. First, it would accelerate the whole assimilation process tremendously, by forming various intermetallics (1,2,9).Secondly, it would protect the high melting point material (i.e., Niobium, Molybdenum, Chromium, Tungsten, Vanadium) from oxidation in cases where alloying is needed for semi-killed steel baths.

The role of exothermicity

It has been observed that for both types of ferroalloys (i.e. class I and class II) exothermicity plays an important role in enhansing the solution rates (5). Two types of exothermicity, namely, Microexothermicity and Macroexothermicity, have been identified. The formation of an intermetallic usually results in a certain amount of heat release. This type of exothermicity, which can be seen in powder alloy compacts, is defined as Microexothermicity. The other type of exothermicity, which a lump of ferroalloy exhibits when it is dissolved into liquid steel is defined as Macroexothermicity. It is associated with the partial heat of mixing of a ferroalloy when it is

dissolved into liquid steel. More details on various types of exothermicity can be found in reference **1.**

Figures 20 and 21 show predictions for the melting times of pure silicon and 50wt% ferrosilicon alloys. In making predictions for these ferroalloys,the shape of the lumps was idealized and considered to be spherical and smooth. These predictions provide conservative estimates of the melting characteristics. That is, any roughness on the surface of the alloy or steel bath resulting from forced convective stirring phenomena will tend to decrease the melting characteristics of these ferroalloys.

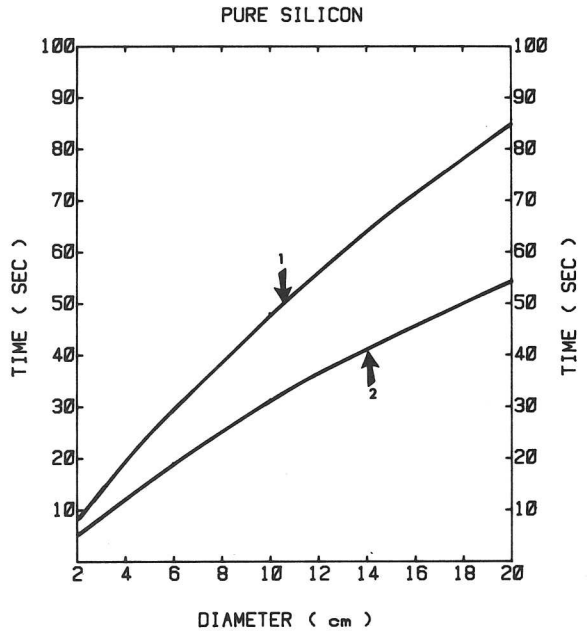

Figure 20: Predicted melting times for pure silicon spheres immersed in liquid steel at 1570°C (curve 1) and 1600°C (curve 2) versus sphere diameter.

Stage and Method for Indroduction of Ferroalloys.

The steelmaking stage at which the ferroalloys are introduced into liquid steel has a significant effect on the recoveries. Ferroalloy additions to the ladle at tap of BOF are aimed at the bottom of the grade chemistry range. The ladle furnace has higher and more reproducible recoveries.This allows the ladle furnace ferroalloy additions to accurately trim to the middle of the grade range while limiting the total bulk addition. Comparative ferroalloy recoveries between the BOF and ladle furnace are given in reference **10.**

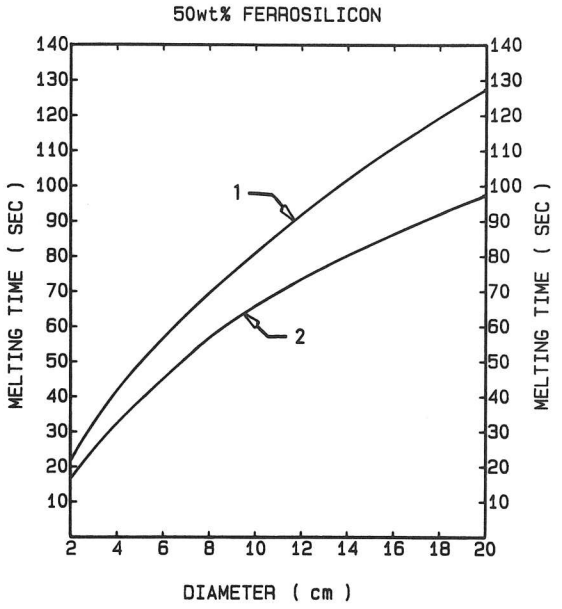

Figure 21: Predicted melting times for 50 wt% ferrosilicon spheres immersed in liquid steel at 1570°C (curve 1) and 1600°C (curve 2) versus sphere diameter.

For the ferroalloys which are light, reactive, or easily oxidized the method of introduction into liquid steel is also important on recoveries. Adding these ferroalloys deep in the ladle minimizes oxidation by air and slag, increases the time and area of contact with the liquid steel and, in some instances ,delays vaporization. It appears that the wire injection technique will be able to introduce the ferroalloys in an optimal manner, so as to achieve the highest recoveries possible. Cotchen **(11)** has indeed presented some data, although not clearly stated how some of the results were derived, that nevertheless support this view.

SOLUTION RATES AND RECOVERIES IN HIGH CARBON LIQUID IRON

The various ferroalloys which are used in high carbon liquid iron can be divided into two classes:

Class I: Ferromanganese, Ferronickel, Ferro-silicon.

ClassII: Ferrochromium Ferromolyb-denum,Ferrovanadium, Ferro-niobium.

The ferroalloys for class I melt in high carbon liquid iron while the ferroalloys for class II dissolve. They follow similar routes described for the case of liquid steel (i.e. Figure 1). The ferroalloys of Class II are expected to follow the route five. This route represents a typical dissolution process. Certain alloy additions from class II dissolve slowly in high carbon liquid iron. To demonstrate this effect, Niobium is an excellent example. Skobls et al[12] added niobium , as ferroniobium, to melt 5 to 7 minutes before pouring and obtained 50% recovery. On the other hand, Campomanes et al [13] claimed that they had achieved a recovery of almost 100% by using powdered (≈100 mesh) ferroniobium and keeping the melt between 1500°C and 1600°C for 15 to 20 minutes. They also mentioned that a much lower recovery resulted from using coarse lumps (25 mm) of ferroniobium.

The expected dissolution times for Class II of conventional ferroalloy lumps are given in reference **2** and summarized in Figure 22 . In this case, the expected dissolution times are given for idealized spherical ferroalloy lumps into high carbon iron bath driven only by natural convection currents. The dissolution in high carbon liquid iron of Microexothermic ferromolybdenum, ferro-chromium, and ferroniobium compacts modified with silicon were also presented in reference **2**. Figure 23 presents the expected dissolution times for silicon modified microexothermic ferroniobium into high carbon liquid iron at 1420 ^{0}C under natural convection conditions. In fact, microexothermic ferromolybdenum and micro-exothermic ferrochromium exhibit similar dissolution times. As seen, there is a dramatic improvement in the dissolution times of microexothermic ferroalloys versus the conven-tional ferroalloy lumps. The microexothermic reaction which takes place during the assimilation of these compacts into high carbon liquid iron is responsible for this enhancement in the dissolution times.

A comparison was made of the recoveries of various ferroalloys dissolving in high carbon liquid iron [2]. Figure 24 shows the observed recovery of Molybdenum in the high carbon iron bath. The circles show the observed recovery of microexothermic additions while the squares present the observed recovery of conventional ferromolybdenum lumps. As seen, the recovery of

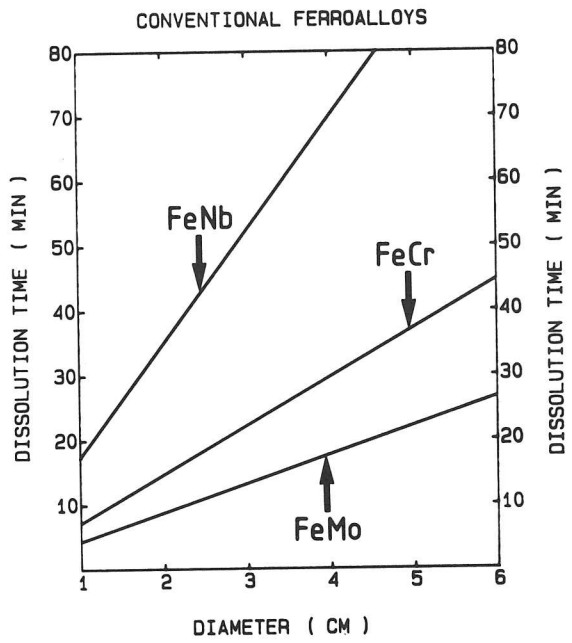

Figure 22: Expected dissolution times of idealized ferroalloy spheres immersed in high carbon liquid iron at a temperature of 1420°C under natural convection conditions.

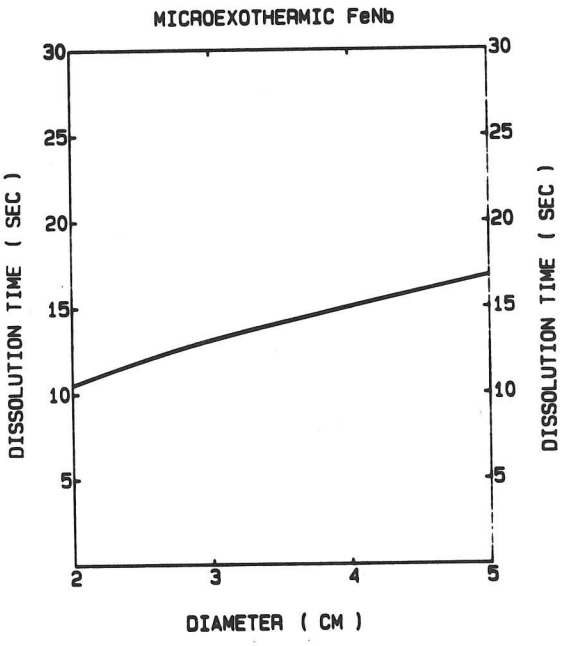

Figure 23: Expected dissolution times of silicon modified microexothermic ferroniobium compacts immersed in high carbon liquid iron at at temperature of 1420°C.

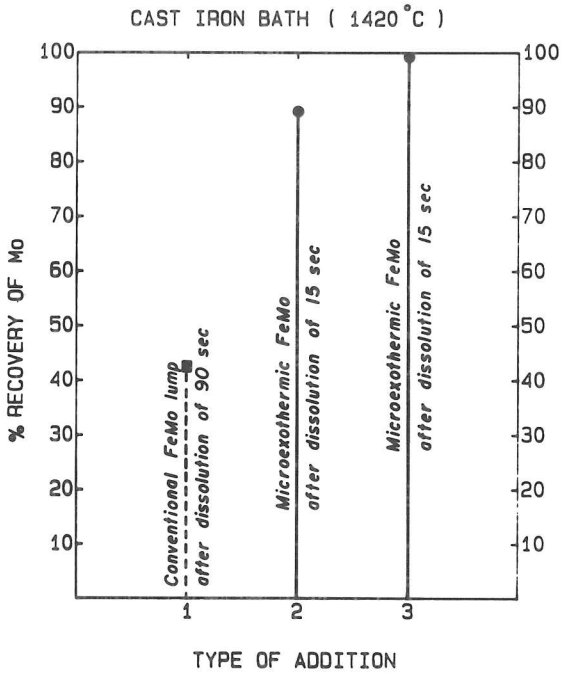

Figure 24: The observed recovery of different types of molybdenum additions in high carbon liquid iron. The circles show the observed recovery of microexothermic ferromolybdenum lumps 6 cm in diameter.

microexothermic additions is substantially higher than the recovery of conventional ferromolybdenum lumps. This can be attributed to the much faster dissolution rate which the microexothermic ferromolybdenum exhibits in the high carbon iron bath than the conventional ferromolybdenum lump. Figure 25 presents a similar result for the observed recovery of chromium in high carbon iron bath. Again here the recovery of microexothermic additions is higher than that of the conventional ferroalloys. Finally Figure 26 illustrates similar results for the observed recovery of Niobium in the high carbon iron bath. One sees here again the recovery of microexothermic ferroniobium additions is higher than the recovery of the conventional ferroniobium lump. It is worth noting at this point that the observed recoveries of microexothermic additions into cast iron refer to dissolution time of 10 sec while recoveries for the conventional ferroalloy lumps refer to dissolution time of 90 sec. In

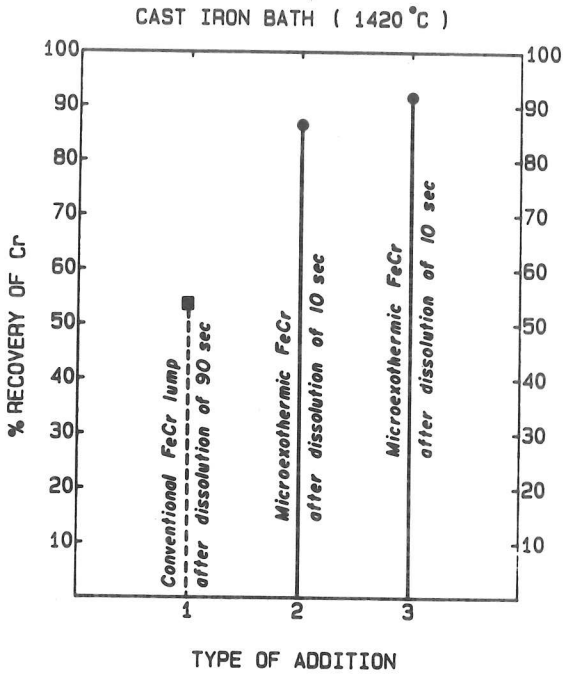

Figure 25: The observed recovery of different types of chromium additions in high carbon liquid iron. The circles show the observed recovery of microexothermic ferrochromium. The square depicts the observed recovery of conventional ferrochromium lumps 3.5 cm.

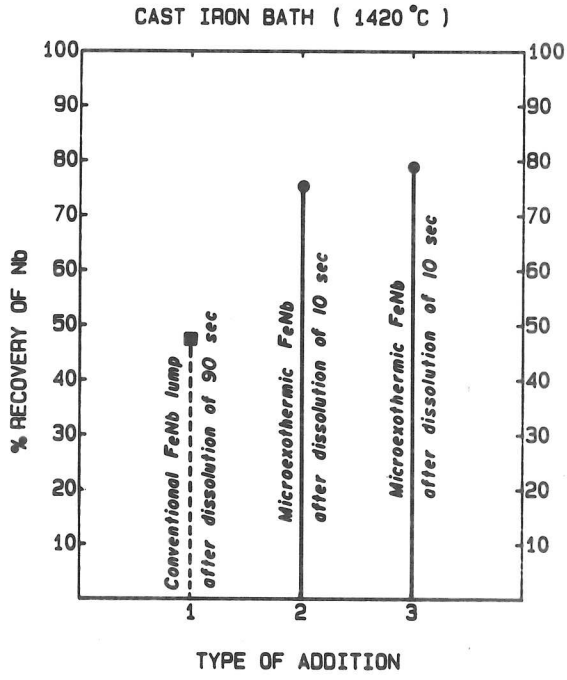

Figure 26: The observed recovery of different types of Niobium additions in high carbon liquid iron. The circles show the observed recovery of microexothermic ferroniobium. The square depicts the observed recovery of conventional ferroniobium lumps 4.5 cm in diameter.

industrial practice, if the microexothermic additions are added in the high carbon iron bath by means of a graphite bell, further improvement is expected in the recoveries.

CONCLUSION

This paper was written to give to both steelmakers and to ferroalloymakers a general idea about the various factors which control the solution rate and recovery of ferroalloys in liquid steel and in high carbon liquid iron. The precise knowledge of all these factors will give to the steelmakers, addition practices with repeatable and consistently high recoveries. In addition, the ferroalloymakers will be able to design new additions which exhibit better recoveries.

REFERENCES

1) S.A. Argyropoulos: "The Effect of Micro-exothermicity and Macroexothermicity on the Dissolution of Ferroalloys in Liquid Steel", Electric Furnace Proceedings, ISS-AIME, vol.42, 1985, pp.133-148.

2) P.G. Sismanis, S.A. Argyropoulos , P.D.Deeley : " The Dissolution of Microexothermic Alloying Additions to Cast-Iron", Electric Furnace Proceedings, ISS-AIME , Vol. 43 ,1986, pp.39-55.

3) S.A. Argyropoulos and G.T.Campbell: "The dissolution Characteristics of Vanadium Ferroalloys in HSLA Steels", Proceedings IV Ferroalloy Congress ILAFA, Brazil , 1988, pp. J1-J9

4) P.G.Sismanis,S.A. Argyropoulos and I.D.Sommerville: " Development of a Facility for Heat and Mass Transfer Studies", W.O.Philbrook Memorial Symposium Proceedings, ISS-AIME , 1988 , pp 193-204.

5) S.A. Argyropoulos: " Dissolution Characteristics of Ferroalloys in Liquid Steel", Iron and Steelmaker , ISS-AIME , November 1984, pp 48-57 .

6) P.G. Sismanis and S.A. Argyropoulos: "The Effect of Oxygen on the Recovery and Dissolution of Ferroalloys", Steelmaking Proceedings ISS-AIME, Vol.69, 1986, pp.315-326.

7) P.G. Sismanis and S.A. Argyropoulos: "The Dissolution of Niobium, Boron and Zirconium Ferroalloys in Liquid Steel and Liquid Iron", Electric Furnace Proceedings, ISS-AIME , Vol. 45, 1987 , pp. 35-48.

8) S.A. Argyropoulos and P.G.Sismanis: " Solution Kinetics of Boron,Niobium and Zirconium Ferroalloys in Liquid Steel", Steel Founders' Research Journal, Number 21, 1988, pp 1-13.

9) J.Shade,S.A.Argyropoulos and A. McLean: "Cored-Wire Microexothermic Alloys for Tundish Metallurgy", Electric Furnace Conference Proceedings, ISS-AIME, Vol. 46, 1988, in press .

10) V.C. Kendrick and R.H. Elder:" Ladle Furnace Applications at the Ashland Works of ARMCO Inc: Temperature and Chemistry Control for Continuous Cast and Ingot Teemed Heats", Electric Furnace Proceedings, ISS-AIME, vol. 42 , 1985 , pp. 219-223.

11) J.K. Cotchen: "Analyzing Ladle Furnace Performance", Iron and Steelmaker, November 1988, pp. 52-58 .

12) T.S. Skobls,N.I. Sandler, V.K. Parenyuk and B.S. Gilman : "The influence of Nb Alloying on Characteristics of Cast Iron", Foundry Production, 7 (1968), pp. 21-22.

13) E. Campomanes and G.Goller: " Effects of Cb Addition on the Properties and Structure of Gray Iron", AFS Transactions 81 (1973) pp. 122-125 .